Journal of Archaeological Science (2001) **28,** 619–631
doi:10.1006/jasc.2000.0602, available online at http://www.idealibrary.com on IDEAL®

The Fractal Dimensions of Lithic Reduction

Clifford T. Brown

6224 Rose Hill Drive, Apartment 2B, Alexandria, VA 22310, U.S.A.

(*Received 26 April 2000, revised manuscript accepted 14 August 2000*)

The fractal distribution is the best statistical model for the size-frequency distributions that result from some lithic reduction processes. Fractals are a large class of complex, self-similar sets that can be described using power-law relations. Fractal statistical distributions are characterized by an exponent, *D*, called the fractal dimension. I show how to determine whether the size-frequency distribution of a sample of debitage is fractal by plotting the power-law relation on a log-log graph. I also show how to estimate the fractal dimension for any particular distribution. Using debitage size data from experimental replications of lithic tools, I demonstrate a fundamental relationship between the fractal dimension and stage of reduction. I also present archaeological case studies that illustrate the simplicity and utility of the method.

Keywords: FRACTALS, LITHIC DEBITAGE, SIZE-FREQUENCY DISTRIBUTION, LITHIC REDUCTION.

Introduction

Lithic debitage is the most ubiquitous and plentiful of all artifacts, and its analysis is of fundamental importance to archaeology. One method of studying debitage consists of evaluating the statistical size-frequency relation of assemblages. This type of analysis was developed by Gunn, Mahula & Sollberger (1976), who studied debitage from the experimental replication of a bifacial tool. They examined the histogram of flake sizes to determine the quantitative characteristics of the debitage from each stage of reduction. This type of sieve analysis is not a substitute for the examination of individual specimens, but it does provide complementary information of significance.

Several statistical methods for the analysis of debitage sizes have been proposed. Patterson (1990), for example, thought that debitage sizes could be effectively modelled using the logarithmic distribution, while Shott (1994) suggested that the log skew Laplace distribution might serve that purpose. The most rigorous study of the debitage size-frequency relation is that of Stahle & Dunn (1982, 1984). They replicated Afton projectile points, a dart point from the North American mid-continent. They segregated the debitage by stage of reduction and then size-graded it using a series of sieves. They compared the resulting empirical frequency distributions to three theoretical ones: the exponential, the Weibull, and the extreme value distributions. Stahle and Dunn concluded that "the Weibull is an accurate model of the size distribution for both flake frequency and weight from biface reduction" (Stahle & Dunn, 1984: 13), "although no clear theoretical connections have been found". The lack of a theoretical basis is a fundamental problem of the Weibull distribution, because it is not informed by any physical theory. For this reason, Weibull himself was obliged to argue in his original paper that "the only practicable way of progressing is to choose a simple function, test it empirically, and stick to it as long as none better has been found" (Weibull, 1951: 293).

I believe that a better function has been found. In this article, I will show that the fractal distribution is a more appropriate and useful model than the Weibull for some size-frequency distributions of debitage. I will explain how to estimate the fractal parameters of empirical debitage distributions. Then I will show how the parameters of experimental debitage distributions are fundamentally related to stage of reduction. Finally, I examine several archaeological test cases that demonstrate the practical utility of the method. It will become apparent that fractal analysis of debitage size distributions is both simpler and more effective than the various methods that have been advocated in the past (e.g., Ahler, 1989; Patterson, 1990; Shott, 1994: 97–98; Stahle & Dunn, 1984).

Fractals

Fractals are a relatively new concept in science—about 30 years old (Mandelbrot, 1967). Although today fractal analysis is extensively employed in the physical, chemical, and biological sciences, it remains a novel concept in many of the social sciences. Fractals are self-similar sets of fractional dimensional. A pattern is self-similar if it composed of smaller-scale copies of itself. One should envision a fractal as an infinite regression of smaller and smaller images that constitute

0305–4403/01/060619+13 $35.00/0

a whole that is similar to its parts. Because of self-similarity, fractals are also "scale invariant", or "scaling". Scale invariance means that they appear (mathematically, if not visually) to be the same at all scales of observation. The fundamental parameter of fractal sets is their fractal (or Hausdorff-Besicovitch) dimension, which, in fractals, is always a fraction, not an integer. Fractals form complex, irregular phenomena like those that predominate in nature. "Clouds are not spheres, mountains are not cones, coastlines are not circles, and bark is not smooth, nor does lightening travel in a straight line" (Mandelbrot, 1983: 1). Fractals are the geometry of non-linear processes, like chaos and self-organized criticality. Thus, they not only accurately and parsimoniously describe natural phenomena, but also indicate the underlying processes that create them. Because fractals have been extensively described in numerous popular works and textbooks (e.g., Batty & Longley, 1994; Mandelbrot, 1983; Schroeder, 1991; Turcotte, 1997) I will not do so here.

A fractal can be any kind of set: points, lines, surfaces, multi-dimensional data, or time series. This paper is concerned mainly with fractal frequency distributions. The concept of the fractal distribution was developed by Mandelbrot (1983: 341–348). Almost any homogenous power-law distribution is fractal because it is the only statistical distribution that does not possess a characteristic or inherent scale (Turcotte, 1997: 1–2). Therefore, they are scale invariant and self-similar, which are the diagnostic qualities of fractals. The number and variety of natural and sociological phenomena that exhibit fractal distributions is almost endless (Schroeder, 1991: 103–120). Fractal distributions include the number–area relation for islands (Mandelbrot, 1975), the size-order relation for streams (Turcotte, 1997: 183–187), the frequency–magnitude relation for earthquakes (Turcotte, 1997: 57–62), the thickness frequency relation for geological strata (Bak, 1996: 78–80), the size-frequency distribution for biological taxa (Burlando, 1990, 1993), Zipf's law of word frequencies (Mandelbrot, 1983: 344–347), Pareto's distribution of incomes (Mandelbrot, 1983: 347–348), and the rank-size distribution of settlements (Batty & Longley, 1994: 48–55; Goodchild & Mark, 1987).

Fractal, or power law, distributions take the general form

$$Y = aX^{b} \tag{1}$$

in which a is a constant and b is the parameter of interest. If one takes the logarithm of both sides of the equation, one obtains:

$$\ln Y = \ln a + b \ln X \tag{2}$$

This is a linear transformation of Equation 1. By plotting the logarithms of the variables, one can obtain an approximation of this linear relationship and thereby estimate the parameters of the power law. I have used natural logarithms in this example, as I will throughout this paper, but one can also use common (base 10) logarithms.

Fractal Fragmentation

Turcotte (1986, 1997; Turcotte & Huang, 1995) has demonstrated that rock fragmentation creates a size-frequency distribution of fragments that obeys the fractal (power law) relation

$$N(>r) = r^{-D} \tag{3}$$

where $N(>r)$ is the number of fragments with a characteristic linear dimension greater than r, and D is the fractal dimension (Turcotte, 1986: 1921, cf. 1997: 42). The exponent D characterizes a specific distribution. It is a measure of the relative abundance of objects of different sizes. It is calculated as:

$$D = -\frac{\ln(N(>r))}{\ln(r)} \tag{4}$$

by taking the logarithms of both sides and solving for D. Turcotte notes that when r is small, the fractal relation is equivalent to the Weibull distribution (1986: 1921; 1997: 42–43), which is itself a power-law distribution (Weibull, 1951).

Turcotte has shown that many natural fragmentation phenomena exhibit fractal distributions with dimensions in the range 1·89 to 3·54 (Turcotte, 1997: 44). Those data sets include broken coal, crushed quartz, disaggregated gneiss, disaggregated granite, glacial till, ash and pumice, terrace sands and gravels, and a variety of other materials. Turcotte analysed two physical models of fractal fragmentation, both of which used the renormalization group approach. Renormalization is a technique that relies upon scale invariance, which in this case was implied by the fractal distribution. The renormalization group models assume that the catastrophic failure associated with fragmentation is caused by the development of fractures. It is noteworthy that a corpus of supporting evidence exists suggesting that geological patterns of fractures are fractal as well (e.g., Barton, 1995; Borodich, 1997; Brown, 1995: 78–79; Hirata, 1989; Korvin, 1992: 127–180; Turcotte, 1997: 67–71; Turcotte & Huang, 1995: 14; Villemin, Angelier & Sunwoo, 1995). It is also believed that the development of microfractures or cracks is implicated in chert fracture (Luedtke, 1992: 75–78). A number of fractal models of fragmentation have recently appeared (e.g., Coutinho, Adhikari & Gomes, 1993; McDowell, Bolton & Robertson, 1996; Mekjian, 1990; Steacy & Sammis, 1991). One of the fundamental strengths of a fractal theory of fragmentation is that it is soundly based in both mathematics and physical theory.

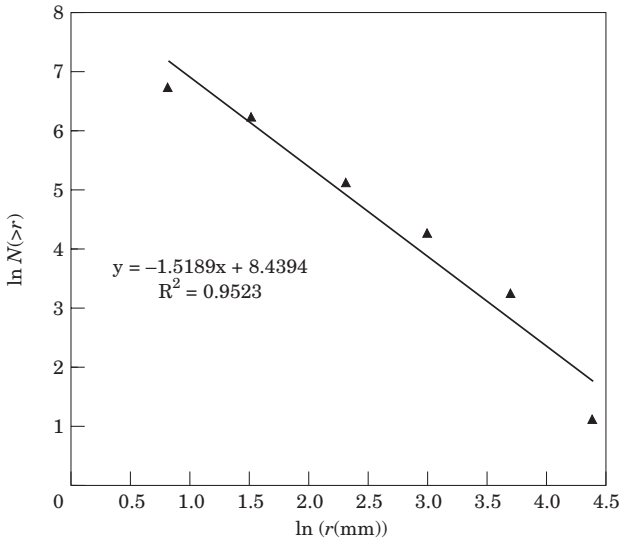

Figure 1. Fractal plot of debitage size—frequency relation for Sollberger Distribution (Gunn, Mahula & Sollberger, 1976).

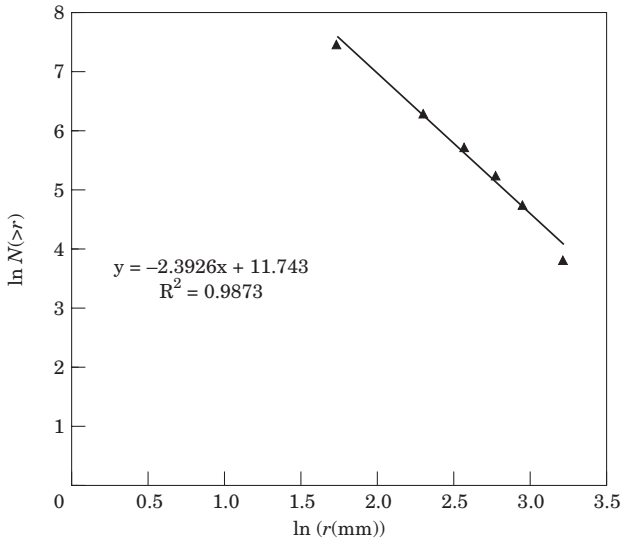

Figure 2. Fractal plot of debitage size—frequency relation for replication of a Clovis Point (Henry, Haynes & Bradley, 1976: 60).

Fractal Dimensions of Debitage

There are several reasons to expect that the process of fragmentation associated with the manufacture of stone tools will yield a fractal size distribution of fragments: (1) as discussed above, it is known that raw materials similar in composition to chert, flint, and obsidian (i.e., quartz, quartzite, ash and pumice) exhibit fractal fragmentation (Turcotte, 1997: 44); (2) the Weibull distribution, which is known to be a good model for some size-frequency distributions of debitage (Stahle & Dunn, 1984), is closely related to the fractal distribution: for small values of r, the Weibull distribution approximates a fractal distribution (Turcotte, 1997: 41); (3) Kennedy & Lin (1986, 1988) have shown that the planform outlines of bifaces are empirical fractal curves, like coastlines and rivers; if the pattern of overlapping flake scars along the edge of a tool forms a fractal curve, it follows that the size distribution of the flakes is fractal as well; (4) similarly, Mecholsky & Mackin (1988) found that the fracture surfaces of archaeological cherts were fractals, the fractal dimensions of which varied with the toughness (K_c) of the chert. Thus, there is reason to believe that chert, obsidian, and other types of stone used to make tools should fragment fractally.

To determine the fractal characteristics of debitage size-frequency distributions, I will start by examining data sets created by experimental knapping of replicas of stone tools, beginning with the original Sollberger distribution presented by Gunn, Mahula & Sollberger (1976). The calculation is illustrated in Table 1. First, one has to calculate $N(>r)$, which from Equation (3), is the cumulative frequency of fragments with a linear dimension greater than r. One sums the raw frequencies in the third column to form a cumulative frequency shown in the fourth column. Then, one calculates the logarithms of both the lower bound of the size interval (r) and the cumulative frequency ($N>$r). One should use the lower bound of the interval as r because the fundamental form of the fractal relation considers the proportion of fragments larger than a given size to the total number of fragments. The lower bound of the interval (or the size of the screen aperture for sieve data) should represent the smallest size debitage in the group.

The next step is to plot the logarithm of the flake size r against the logarithm of the cumulative frequency $N(>r)$. The plot of these data is shown in Figure 1. For the relation between the two variables to be fractal, this plot must be linear. If it is, the slope of the least squares regression line provides an estimate of D. Thus, from Equation 4 we have $D=1{\cdot}52$, which is merely the negative of the slope. This is the fractal dimension of the original "Sollberger distribution". The coefficient of determination, the statistic that measures the proportion of the variation in the data explained by the regression, is a comfortably high 0·95, or 95%. This demonstrates that the relation is highly linear, because it is almost perfectly modelled by the linear regression. The significance of the regression, taken from the analysis of variance table, is $P=0{\cdot}000867$.

Gunn and his colleagues understood the type of statistical distribution they had discovered: "[T]he curve is continuously rising and approaches infinity as the shatter approaches the crystalline grain size of the stone" (1976: 5). And, they explained it correctly, though not quantitatively. "It is generally understood by flintknappers that when a flake is removed smaller flakes are simultaneously struck, mostly off the platform of the larger flake. It seems reasonable that these simultaneous removals would be much smaller than the main flake, probably measuring in the very small Classes 5 and 6, 2·25–10 mm. What the ratio of main

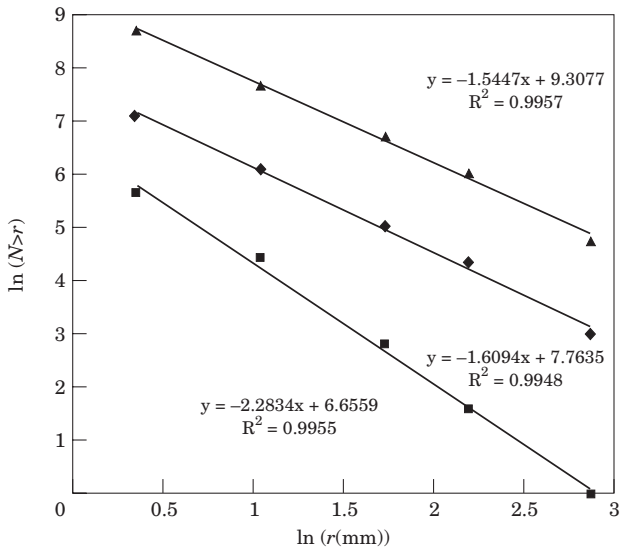

Figure 3. Fractal plot of debitage size—frequency relation for three experiments (Baumler & Downum, 1989). ◆, Exp 1; ▲, Exp. 5; ■, Exp. 19.

flakes to simultaneous flakes would be is conjectural at this point'' (1976: 6). The fractal dimension quantifies the conjectural ''ratio of main flakes to simultaneous flakes''.

Other experimental data sets can be used to examine the fractality of size distributions of debitage (Table 2). Henry, Haynes & Bradley (1976: 60) published debitage size-frequency data from the replication of Clovis points. In Figure 2, I plot the fractal relation for that data set. Note that the dimension $D=2{\cdot}39$ is very different from that of the first example. The variability of D between the two data sets suggests that D is capturing a fundamental quality of the distribution, one that can perhaps be used to characterize assemblages of debitage. I will further examine this property for data sets from different reduction sequences with other end products.

Both of the data sets examined above derive from debitage from bifacial reduction of projectile points. Other reduction trajectories also produce fractal distributions of debitage sizes. In Figure 3, I plot the fractal relation for three experimental replications conducted by Baumler & Downum (1989). Experiments 1 and 5 consisted of ''reduction of previously decorticated, medium-sized nuclei (*c*. 8–15 cm maximum dimension), for the purpose of generating blades or elongated flakes between 4 and 8 cm long''. Experiment 19 was one of several described as: ''flakes and blades of various sizes and shapes were selected for unifacial retouching, producing what is commonly referred to as 'scraper' retouch on one or more edges of the blanks'' (1989: 103). First, the linearity of the relations shown in Figure 3 indicates that they are fractal. Thus, non-bifacial reduction trajectories also produce fractal size distributions of debitage. Second, the fractal dimensions for Experiments 1 and 5 ($D=1{\cdot}61$, and $D=1{\cdot}54$, respectively) are similar, while that for the scraper production, Experiment 19, is different from the first two ($D=2{\cdot}28$). This also suggests that similar trajectories result in similar fractal dimensions. Table 2 shows that many experimental and ethnoarchaeological data sets yield fractal relations.

Table 2 lists the fractal dimension (D), the coefficient of determination (r^2), and the probability (P) associated with a number of experimental data sets, including those discussed above. In general each data set represents a single replication of some sort of stone tool. In a few cases, the data set resulted from multiple replications of a similar reduction process (e.g., Behm, 1983; Henry, Haynes & Bradley, 1976) or from mixed debitage from many experiments (Fladmark, 1982). The next columns in the table list, in abbreviated form, the raw material and the reduction trajectory as described by the original authors. The reader is urged to consult the original sources for more detail.

Not surprisingly, within this large number of experiments there was significant methodological variability. Different methods of measuring specimens appear to produce different results, and, therefore, the experiments are not all directly comparable. The different methods appear to have little effect, however, on the fractality of the relation. That so many of these replications, produced by many different artisans, yield clear fractal relations is a strong indication of the robustness of the technique.

Table 1. Variables for the fractal plot of the Sollberger Distribution

Size interval (mm)	Lower bound (r)	Frequency	Cumulative frequency ($N>r$)	ln (r)	ln ($N>r$)
2·25–4·49	2·25	351	873	0·8109	6·7719
4·49–10	4·49	349	522	1·5019	6·2577
10–20	10	101	173	2·3026	5·1533
20–40	20	46	72	2·9957	4·2767
40–80	40	23	26	3·6889	3·2581
>80	80	3	3	4·3820	1·0986

Table 2. Parameters for various reduction trajectories

Experiment	D	r^2	P	Experiment type	Material type	Notes	Reference
A1	1·35	0·9911	0·004	Cobble testing	Knife River Flint	Mean data from 37 replications	Ahler, 1986
A2	2·23	0·9721	0·014	Hard Hammer Freehand Percussion	Knife River Flint	Mean data from 25 replications	Ahler, 1986
A3	2·80	0·9841	0·009	Bipolar Core	Knife River Flint	Mean data from 30 replications	Ahler, 1986
BD1	2·80	0·9841	0·009	Flakes and blades from core	Wreford Chert		Baumler & Downum, 1989
BD2	1·84	0·961	0·020	Flakes and blades from core	Wreford Chert		Baumler & Downum, 1989
BD3	1·17	0·9935	0·003	Flakes and blades from core	Wreford Chert		Baumler & Downum, 1989
BD4	1·49	0·998	0·001	Flakes and blades from core	Alibates Chert		Baumler & Downum, 1989
BD5	1·54	0·9957	0·000	Flakes and blades from core	Government Mountain Obsidian		Baumler & Downum, 1989
BD6	1·72	0·9888	0·006	Flakes and blades from core	Government Mountain Obsidian		Baumler & Downum, 1989
BD7	1·65	0·9712	0·015	Unifacial scraper from flake or blade	Wreford Chert		Baumler & Downum, 1989
BD8	1·64	0·9979	0·001	Unifacial scraper from flake or blade	Wreford Chert		Baumler & Downum, 1989
BD9	2·21	0·9726	0·014	Unifacial scraper from flake or blade	Wreford Chert		Baumler & Downum, 1989
BD19	2·28	0·9955	0·000	Unifacial scraper from flake or blade	Alibates Chert		Baumler & Downum, 1989
BE1	1·40	0·9966	0·002	Hard hammer (HH) reduction of large cores to produce large flake blanks	Galena Chert		Behm, 1983
BE2	1·65	0·9744	0·013	Soft hammer (SH) reduction of large cores to produce large flake blanks	Galena Chert		Behm, 1983
BE3	1·83	0·9736	0·013	HH reduction of small cores to produce small flake blanks	Galena Chert		Behm, 1983
BE4	1·92	0·9753	0·012	SH reduction of small cores to produce small flake blanks	Galena Chert		Behm, 1983
BE5	1·88	0·9805	0·010	HH edging of flake blanks to produce stage 2 bifaces	Galena Chert		Behm, 1983
BE6	1·91	0·9673	0·016	HH edging of nodules to produce stage 2 bifaces	Galena Chert		Behm, 1983
BR1	2·97	0·9623	0·003	Bayogoula arrow point	Oolitic chert gravel from Citronelle Frm. (Mississippi)		Brown *et al.*, 1995
C2	1·88	0·9281	0·008	Started with tested cobbles to prepared blade cores to arrow points	Local residual chert cobbles in Chiapas, Mexico	Ethnoarchaeological samples from Lacandones	Clark, 1991: Table 2
C4	1·98	0·9465	0·005	Started with tested cobbles to prepared blade cores to arrow points	Local residual chert cobbles in Chiapas, Mexico	Ethnoarchaeological samples from Lacandones	Clark, 1991: Table 4
C5	1·79	0·9676	0·003	Started with tested cobbles to prepared blade cores to arrow points	Local residual chert cobbles in Chiapas, Mexico	Ethnoarchaeological samples from Lacandones	Clark, 1991: Table 5
F1	0·38	0·9928	0·004	Mixed samples from practice knapping	Varied/mixed	All quadrants combined	Fladmark, 1982
G1	1·52	0·952	0·001	Basally-notched biface	Chert nodule		Gunn *et al.*, 1976
H1	2·39	0·9873	0·000	Clovis point	Chert of unknown origin		Henry *et al.*, 1976
K1	1·30	0·9657	0·017	Bipolar split cobble	Quartz stream cobble		Kalin, 1981
K2	1·99	0·9947	0·003	Bipolar split cobble	Quartz stream cobble		Kalin, 1981
K3	2·09	0·9965	0·002	Split cobble, made 1 failed biface and 1 stemmed point	Quartz stream cobble		Kalin, 1981
R1	2·35	0·969	0·016	Biface edging	Knife River Flint		Root, 1997
R3	2·85	0·9613	0·020	Expert biface thinning	Knife River Flint		Root, 1997
R4	1·36	0·9903	0·005	Cobble testing	Knife River Flint		Root, 1997
R5	2·07	0·9719	0·014	Unprepared core	Knife River Flint		Root, 1997
R6	2·39	0·9651	0·018	Prepared core	Knife River Flint		Root, 1997
R7	2·65	0·9816	0·009	Bipolar core	Knife River Flint		Root, 1997
S2	3·12	0·9661	0·000	Afton Projectile Point	Local chert from Boone Frm.		Stahle & Dunn, 1984
S4	3·11	0·9602	0·001	Afton Projectile Point	Local chert from Boone Frm.		Stahle & Dunn, 1984
S5	3·33	0·9658	0·000	Afton Projectile Point	Local chert from Boone Frm.		Stahle & Dunn, 1984
S6	2·72	0·9883	0·000	Afton Projectile Point	Local chert from Boone Frm.		Stahle & Dunn, 1984
S7	2·62	0·9885	0·000	Afton Projectile Point	Local chert from Boone Frm.		Stahle & Dunn, 1984
S8	2·57	0·9516	0·000	Afton Projectile Point	Local chert from Boone Frm.		Stahle & Dunn, 1984
S10	2·82	0·9767	0·000	Afton Projectile Point	Local chert from Boone Frm.		Stahle & Dunn, 1984
S12	2·58	0·9808	0·000	Afton Projectile Point	Local chert from Boone Frm.		Stahle & Dunn, 1984

The data sets in Table 2 were restricted to ones that fit the fractal model well. This was done by selecting those that produced significant regressions, which ensures that they are linear relations. An arbitrary level of significance was set for the regressions at $\alpha = 0.02$. This requirement tends to exclude data sets in which the debitage was grouped into a small number of size intervals, because when calculating the fractal relation each size category forms a case in the regression; consequently, the more size intervals (i.e., the more sieves), the more robust the regression because of the larger number of cases. Thus, with only three or four measured size intervals, a relation has to be almost perfectly linear to be significant. This is true for any distribution: modelling will only be meaningful with a reasonable number of size intervals ranging across as many orders of magnitude as possible. The use of only three or four size intervals seriously weakens some published analyses of debitage size distributions.

The data in Table 2 demonstrate the fundamental relationship between the fractal dimension and stage of reduction. Most reduction trajectories proceed from coarser to finer work. Coarser work involves higher loads and results in the removal of larger flakes on average than the finer work of the later stages. Consequently, it is generally accepted that earlier stages of reduction produce proportionately more large flakes while later stages generate an increasing proportion of smaller flakes. When using the fractal dimension to compare stages of reduction, therefore, one should expect that D will increase with later stages of reduction. The data in Table 2 bear out this conclusion. For example, the first six experiments by Baumler & Downum (1989) shown in the table (BD1–BD6) represent an earlier stage of reduction than the remaining four (BD7–BD9, BD19). The mean value of D for the first six is 1·56, while for the later four the mean is 1·945. Similarly, the first two replications listed for Behm (1983) (BE1–BE2) represent an earlier stage of reduction than the other four listed (BE3–BE6). The first two have lower values of D than the remaining four. A similar situation obtains for experiments K1–K3: splitting a cobble (K1–K2) is an earlier stage of reduction than splitting a cobble and creating a projectile point (K3) (Kalin, 1981). Again, among Root's replications (R1–R7) (Root, 1997), there is a progression of stages that is generally paralleled by an increase in the value of D: "cobble testing" exhibits the lowest value, "unprepared core reduction" is lower than "prepared core reduction", and so forth. Another example of this pattern comes from Ahler's work (1986: 64–66, Table 13). Cobble testing, again, has the lowest value of D, hard hammer free-hand percussion the next highest, and soft hammer bifacial thinning the highest. Finally, the highest values of D in Table 2 are associated with production of Bayogoula and Afton points, both of which are finely wrought bifaces. In sum, there is a natural and systematic relationship between fractal dimension and stage of reduction.

Archaeological Case Studies

A small number of archaeological examples will illustrate the practical utility of fractal analysis of debitage for the archaeologist. The examples have been chosen to demonstrate how the fractal dimension relates to stage of reduction and also to show how fractal analysis can contribute to archaeological interpretation of lithic assemblages.

Methods

The size grading of the debitage in all the following examples was performed, at least in part, by measuring the "maximum dimension" of each specimen. This process consisted of matching each specimen, by hand, to the smallest circle or square of a graduated series within which it fit. For the purposes of these analyses, the next smaller size is considered the sieve aperture upon which that specimen would have rested. There is a small fallacy in this approach, however, because in theory sieves sort pieces by their intermediate axis, while our measurements were based upon the largest axis. This fact does not invalidate the following analyses, but it means that the results will differ from analyses conducted with graduated sieves.

In addition, all these archaeological distributions have been affected by their method of recovery. In particular, the small size materials have been irregularly recovered; the incomplete recovery results from the sieving of soil through screens during excavation. As the minimum dimension of an artifact approached the aperture of the excavation screen, the likelihood that it fell through the screen increased, regardless of the artifact's maximum dimension. This explains why in some cases the number of flakes occurring in the smaller sizes is less than would be predicted by the fractal relation. For example, in the excavations carried out at Mayapán (see below), we employed 1/4-inch hardware cloth for sieving. The size of the square aperture is therefore *c.* 6·35 mm, but along the diagonal the aperture is about 9 mm. In theory, we should not have recovered anything smaller than 9 mm, but of course we did. More important, some significant proportion of debitage larger than 9 mm in maximum dimension must have passed through the screen because its smallest axis fit through the aperture. Therefore, our smallest size grades are missing specimens that slipped through the excavation screen. This forced us to exclude data from the smallest size grades because they were inconsistently recovered, and their frequencies skewed the results.

The use of graduated sieves for granulometry, which is the origin of the measurement techniques used here, were designed by geologists for the description of natural sediments. They therefore rely in some respects on the natural tendency of geological particles to approach a spherical form. For example, the ability of geologists to convert from particle counts of given radii

to masses depends on the assumption that particles are approximately spherical. Of course, the particle shapes of natural sediments are highly distinctive, and the study of them is well developed. Lithic tool debitage is, in contrast, a very different kind of phenomenon.

Most debitage is distinctively unnatural in shape. Not only do most specimens exhibit attributes that are rare in nature, like bulbs of percussion, faceted or prepared platforms, and so forth, but many flakes are unnaturally thin and flat. This tendency derives from the exploitation of the properties of conchoidal fracture to transform the natural shape of the material into an implement useful to humans. The tendency of flakes to be tabular rather than spherical contributes to the difficulty of accurately and consistently performing sieve analyses on this type of material. It implies that for studies such as these hand measurement of individual specimens is preferable to the use of sieves; nevertheless, in the future it would be worthwhile to experiment with hand measurement methods that logically mimic sieving methods.

The Wetherington Island Site (8HI473)

The Wetherington Island Site is a large, stratified, multicomponent site located near the eastern edge of Tampa, Florida (Brown *et al*., 1996; see also Chance, 1982; Chance & Misner, 1984; Goodyear *et al*., 1983). It lies along the north bank of Cow House Creek, which flows seasonally in an abandoned channel of the Hillsborough River. The site is one of a large cluster of related and contemporaneous sites located on the landform between Cow House Creek and the Hillsborough River. The main component of the site is a massive, stratified deposit of debitage derived from quarrying of residual chert nodules and bedrock cherts from the Tampa Limestone Member of the Hawthorne Formation. Excavations revealed quarry pits, unmodified chert nodules, and modified bedrock cherts. The cherts at the site include fossilized coral as well as more common types of chert and chalcedony. The main component is poorly dated, but a small number of identifiable projectile points indicate that it falls in the Middle and Late Archaic periods. The major occupation is preceded by a deeply buried, fugitive component associated with megafauna. This earliest component is presumably Paleoindian. The latest component was deposited after the Hillsborough River, having burial the main component under alluvial sands, abandoned the Cow House Creek channel in response to rising Holocene sea level. Cow House Creek became a seasonal overflow channel for the new Hillsborough River course. The underfit creek meandered in the oversized channel, slowly filling it with a complex series of interbedded sands and clays. In this period, people camped repeatedly along the edge of the slough, depositing materials within the slowly accreting sediments. This youngest component that developed in the infilling channel appears to be functionally different from the adjacent quarrying site. There is little evidence for chert exploitation or knapping beyond what might occur in any hunting camp (Brown *et al*., 1996).

The main component is characterized by enormous quantities of debitage, including large cores measuring over 1 m in length. This component of the site is obviously a lithic procurement and primary reduction locus. The evidence for this conclusion takes several forms. First, we excavated at least one quarry pit and exposed parts of a couple of others. Second, we identified areas where bedrock cherts had been exploited. Third, we found unmodified chert nodules, along with many modified fragments and cores. Fourth, the percentage of cortical debitage was quite high. Fifth, the average size of flakes, as measured by weight, was large. These are all indicia of lithic raw material extraction and primary reduction. Nevertheless, there is some internal variation and spatial structure within this component. Quarry pits seem concentrated in some areas, while knapping and reduction took place in other areas (Brown *et al*., 1996).

The quantity of debitage recovered from the excavations precluded analysis of every specimen. Only selected proveniences were analysed fully, and, when the number of artifacts from a single provenience was large, a random sample of debitage was drawn for analysis. The maximum dimension of each specimen was measured by using a series of graduated circles on a template to assign specimens to bins. For debitage measuring 54 mm or less, the increment between circles was 4·5 mm; thereafter, the increment was 18 mm (Brown *et al*., 1996: 130–132)

Block D exhibited complex stratigraphy, but the discovery of quarried chert bedrock at the bottom of the excavation suggested that the matrix consisted of mixed feature fill within a large quarry pit. The debitage from the unit clearly indicates an early stage of reduction: the mean weight of specimens, the percentage of specimens with cortex, and the percentage shatter are all high (Table 3). Figure 4 presents the fractal plot of the size-frequency relation for a random sample of debitage from Block D, Unit 9, Level 5. The low value of D, 1·4, indicates an early stage of reduction that is in agreement with the other characteristics of the specimens. For comparison, note that Experiment A1, "cobble testing" (Table 2), has a fractal dimension of 1·35. Similarly, Experiment R4, cobble testing of Knife River Flint, has a fractal dimension of $D = 1{\cdot}36$. Experiment BE1, "hard hammer reduction of large cores to produce large flake blanks", has a fractal dimension of 1·40. All those reduction trajectories appear to be reasonable descriptions of the behaviour found at Block D of Site 8HI473.

The debitage samples analysed from Block G exhibited characteristics similar to those from Block D (Figure 5). Again, the mean weight, percent with cortex, and percentage of shatter all point to an early stage of reduction (Table 3). The value of the fractal

Table 3. Summary characteristics of debitage from selected proveniences at the Wetherington Island Site

Provenience	Mean weight of debitage (g)	Percentage with cortex	Percentage of shatter	*D*	Stage of reduction
Block D, Unit 9, Level 5	7·65	59·76	12·8	1·4	Very early
Block G, Unit 15, Levels 3–6	10·67	46·32	8·4	1·85	Very early
Block E, Unit 17, Level 3, Feature 11–1	1·22	15·89	1·3	2·5	Early to middle
Block H, Unit 20, Level 5	0·74	32·86	8·6	2·9	Middle

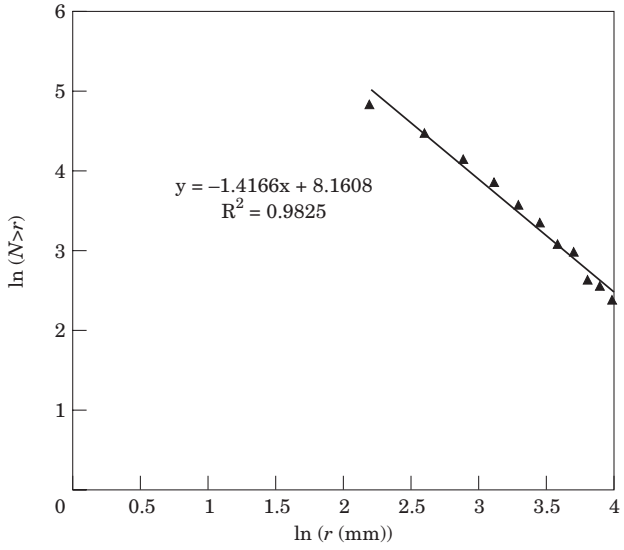

Figure 4. Fractal plot of debitage size—frequency from Block D, random sample, site 8HI473 (Brown *et al.*, 1996).

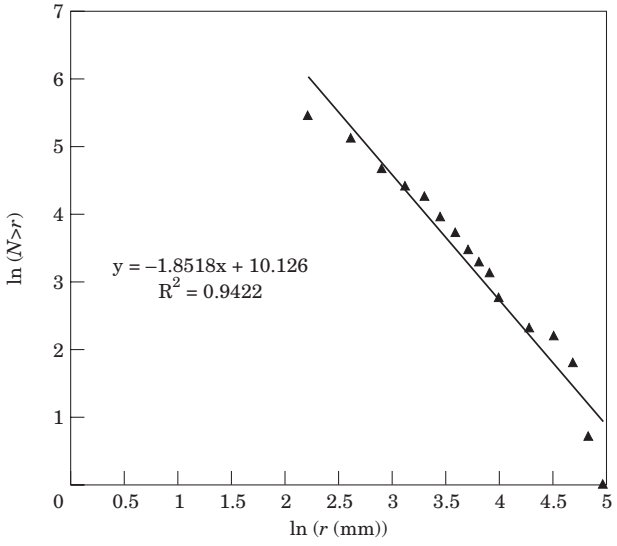

Figure 5. Fractal plot of debitage size—frequency relation from combined random samples, Block G, Site 8HI473 (Brown *et al.*, 1996).

dimension, $D=1{\cdot}85$, also corresponds to an early stage of reduction.

A sample of debitage from Block E, Feature 11–1, a workshop and primary reduction locus, has distinctly different characteristics: flake weight, percent with cortex, and percentage of shatter are all dramatically lower. *D* is correspondingly higher, 2·5, which indicates a measurably later stage of reduction (Figure 6).

The final sample, from Block H, represents the latest component at the site, from the infilled channel of the ancestral Hillsborough River. Although the percent of debitage with cortex and proportion of shatter are moderate, the low average specimen weight (0·74 g) unambiguously indicates a later stage of reduction than the other samples (Table 3). The associated fractal dimension is 2·9, which suggests a secondary or intermediate stage of reduction (Figure 7). We know relatively little about this occupation of the site, but it resembles a base camp or hunting/foraging station much more than it does a specialized lithic procurement site (Brown *et al.*, 1996: 252–256).

In this section, I have shown (1) that data sets from archaeological assemblages of debitage are fractal distributions; (2) that the fractal analysis of archaeological debitage produces results that correspond to the expectations derived from the analysis of the experimental data sets. Specifically, the values of *D* for archaeological collections approximate those from experiments that replicate behaviours that are inferred in the archaeological cases; and (3) equally important, that the values of *D* from the archaeological data sets confirm the interpretations of stage of reduction derived from conventional measures, like mean weight of specimens.

Mayapán (16Qd(7):2)

Mayapán, Yucatán, México, is a Late Postclassic period site located approximately 40 km south–southeast of Mérida, the state capital. The site was culturally Lowland Maya, but exhibits the strong central Mexican influences characteristic of that period in the Peninsula of Yucatán. The site, which is immediately pre-Conquest in date (*c.* AD 1200 to 1450), is well-known historically as the political capital of northern Yucatán. It is a large site, occupying more than 4 km^2, and is surrounded by a massive defensive wall over 9 km long. Within the wall, the ruins of over 4000 buildings are found (Brown, 1999; Smith, 1962).

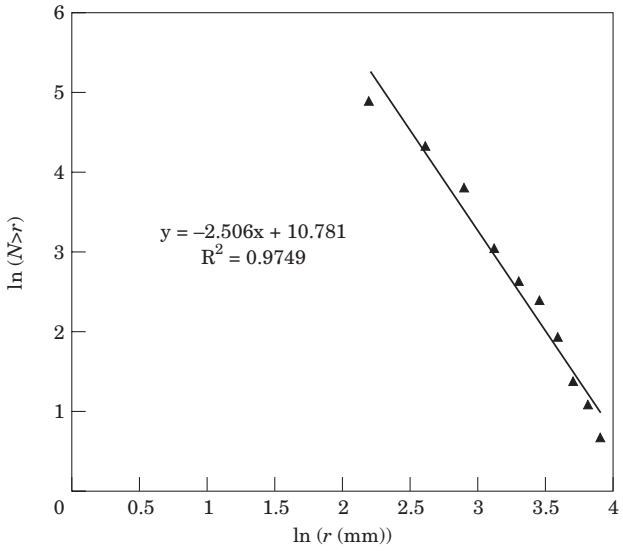

Figure 6. Fractal plot of debitage size—frequency relation from Block E, unit 17, level 3, feature 11-1, site 8HI473 (Brown *et al.*, 1996).

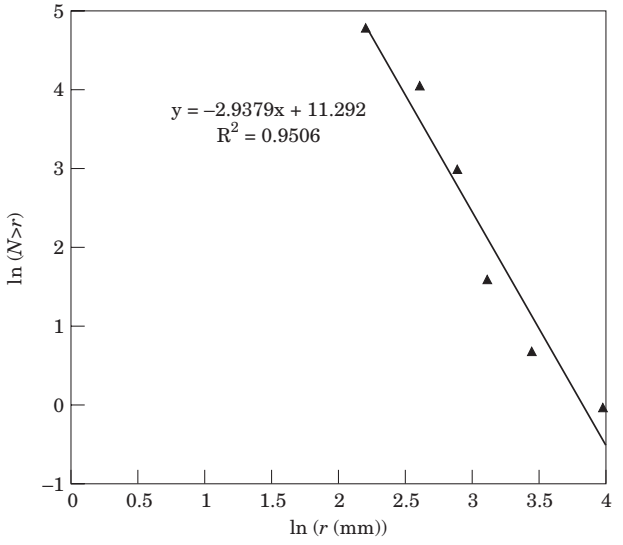

Figure 7. Fractal plot of debitage size—frequency relation from Block H, level 5, site 8HI473 (Brown *et al.*, 1996).

Both chert and obsidian lithic industries are known from the site, but here I am only concerned with the former.

The broad outlines of the chert assemblage of Mayapán have been described by Proskouriakoff (1962). Formal bifaces are known from the site, but are rare outside of ceremonial contexts. In my excavations in residential contexts, I found that expedient chert tools are common, while formal or curated tools are the exception. The total absence of any kind of functional axe or celt in the assemblage is noteworthy. The appearance of small, side-notched chert arrow points seems to be related to the Mexican influence in the region.

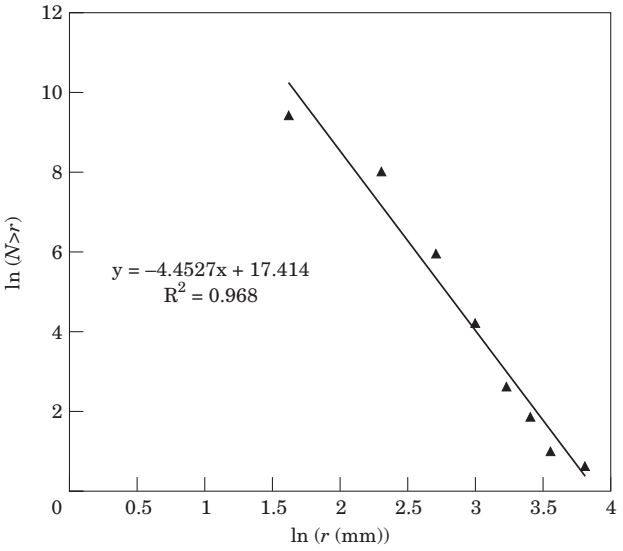

Figure 8. Fractal plot of the size-frequency relation of debitage from chert workshop in Houselot S-139, Mayapan (N=12,821).

For some chert artifact samples, I measured the maximum dimension of each specimens by using a series of square templates that increased in size in 5 mm increments, as measured along the side, not the diagonal, of the square. I size-graded the materials by determining which square the artifact could fit in without touching the sides of the square (Patterson, 1990). I applied this technique to the thousands of specimens recovered from systematic surface collections from a chert workshop in Houselot S-139 (see below). For other specimens, mainly those specimens recovered from excavations, I measured their maximum dimensions to *c.* 0·1 mm using calipers. For the purposes of the analyses presented here, those ratio scale measurements have been sorted into a series of bins. The bins have been kept fairly narrow (i.e., 2 mm) so as not to degrade the data more than necessary. Since the analysis of the chert assemblage is incomplete, these results should be considered preliminary.

In the northeastern portion of Houselot S-139, I identified a chert workshop. It appeared to be a workshop in part because of the high surface density of chert (in excess of 1000 m^{-2}) (Brown, 1999: 460–461). Compared to material from other proveniences, the debitage from the workshop was distinctive. For example, the workshop contained an unusually large number of biface thinning flakes. In addition, the debitage from the workshop had more non-cortex and fewer cortical specimens than expected when compared with material from other households (χ^2=26·63, df=2, P=1·65 × 10^{-6}) (Brown, 1999: 460–462). The fractal relation between size and frequency for the debitage is shown in Figure 8: D=4·5 (r^2=0·97, P=1·0 × 10^{-5}). This value of D is higher than any recorded from experimental replications. It reflects a high proportion of very small flakes and a corresponding dearth of

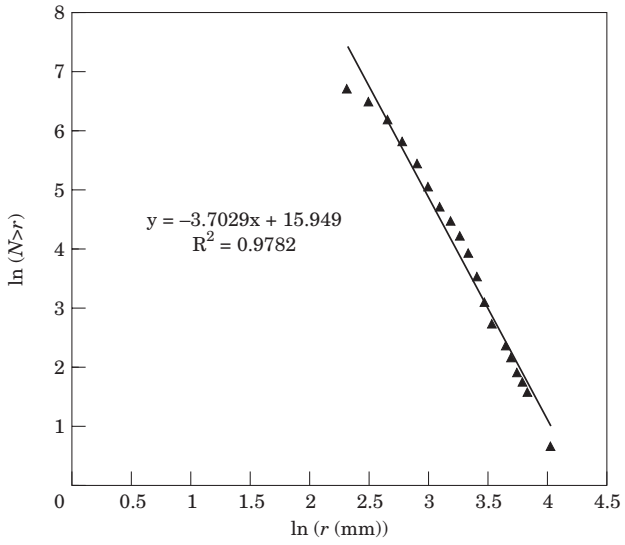

Figure 9. Fractal plot of size—frequency relation for debitage from pit 17 and random surface collections (for $r>10$ mm), Houselot S-139, Mayapan.

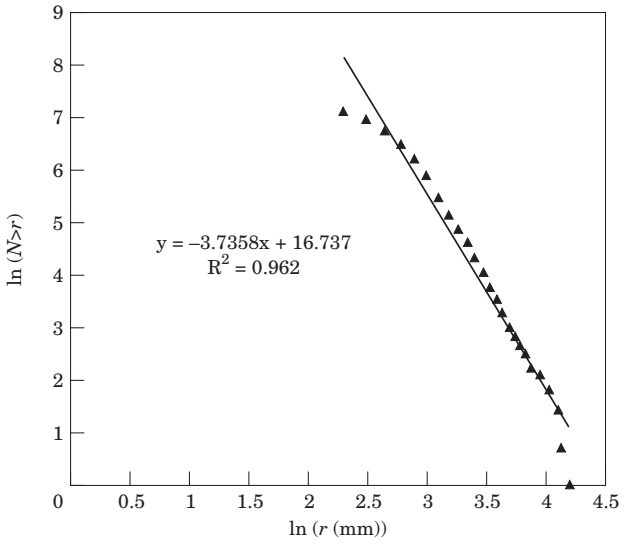

Figure 10. Fractal plot of size—frequency relation for debitage from Houselot S-130, Mayapan.

large ones. This could occur as a result of either the reduction of small pieces of raw material, that is, starting from small nodules, or very late stage reduction, or a combination of both. One might argue that this is a lag deposit from cleaning and removal of secondary refuse, a process which is known to create lag deposits of tiny particles (e.g., Behm, 1983; Clark, 1991*a*, *b*; Healan, 1995). This argument has to be rejected, however, because of the frequency of large fragments in the workshop; that is, while the average size of debitage in the workshop is small, the number and size of the large fragments present make it unlikely to be a lag deposit. Rather, the large numbers of biface thinning flakes and the high value of D both point to primary refuse from late stage biface reduction and finishing. The volume of production that can be inferred for this workshop is clearly in excess of that which could be consumed within the household and therefore must be interpreted as mass production or production for exchange.

Another group of samples from similar contexts within the same houselot (i.e., Pit 17 and random surface collections) provide generally similar results (Figure 9). For this data set, $D=3{\cdot}7$, $r^2=0.98$, and $P=1{\cdot}5\times10^{-15}$. Although the technological emphasis at Mayapán is clearly on expedient industries, the formal bifaces, recovered mainly from ceremonial contexts at the site centre, are finely manufactured. Accordingly, it is possible that this workshop served to finish bifaces of one or more of the types found in the ceremonial centre.

Houselot S-130 lies near Houselot S-139. Excavations in Houselot S-130 produced unusually large quantities of chert compared to most houselot excavations. The fractal dimension is shown in Figure 10: $D=3{\cdot}7$, $r^2=0.96$, and $P=7{\cdot}72\times10^{-18}$. The fractal dimension D for Houselot S-130 is remarkably similar to those of Houselot S-139, and most of the observations made above apply to both. The overall volume (and density) of chert debitage in Houselot S-130 is, however, much lower than in S-139; therefore, it seems unlikely that houselot S-130 can boast of specialized production.

Most of the other houselots investigated at Mayapán did not exhibit a fractal distribution of debitage. The raw data from those houselots (i.e., the frequencies in the size intervals, not the cumulative frequencies) presented an approximately normal (Gaussian) frequency distribution. This is inexplicable in terms of current theories of fragmentation, but is easy to understand archaeologically: redeposition must have caused the loss of many small flakes. It is well-documented that cleaning and re-disposal of knapping debris tends to leave small flakes behind in primary contexts as a lag deposit (e.g., Behm, 1983; Clark, 1991*a*, *b*; Healan, 1995). Thus, small flakes remain near their original locations as primary refuse while a disproportionate number of larger flakes are removed and transported to become secondary refuse.

The data from Mayapán confirm, again, that the fractal analysis of archaeological collections yields meaningful inferences about stage of reduction and provides a useful method of describing the size distribution of assemblages of debitage.

Conclusion

I have argued that since most rock fractures fractally, then so too should the rocks used by people to make stone tools. I have shown that experimental replications of stone tools create fractal size-frequency distributions of debitage. Moreover, the parameter of

the fractal distributions (the fractal dimension) relates closely and systematically to stage of reduction. This discovery implies that the method is robust and useful. The archaeological cases examined here confirm that the method has inferential power and practical applicability. Finally, it should be apparent that the method of evaluating the fractal parameters is very simple and accessible to all archaeologists. The method presented here is the best way to evaluate the relative proportions of flakes of different sizes: D is the best and easiest measure of this variable. It is mathematically correct and supported by physical theory.

Not all debitage distributions are fractal, but many are. The fractal distribution is clearly the natural size-frequency distribution for the fragmentation of most archaeological lithic materials. The relationship of the fractal dimension to stage of reduction is fundamental and systematic and should be exploited by archaeologists. The fractality of this phenomenon appears to be largely a function of geophysics, but it is clearly influenced by human behaviour, as the variation of D shows.

A general and significant reason for adopting fractal analysis is the implications it carries for non-linear science in archaeology. Fractal patterns are the result of strongly non-linear dynamics, particularly of systems that are chaotic or self-organized critical (SOC).

Whereas a fractal is always a set, chaos is a characteristic of deterministic dynamical systems. Chaotic systems are common in nature, perhaps more common than stable, non-chaotic ones. A deterministic dynamical system is said to be chaotic if "solutions that have initial conditions that are infinitesimally close diverge exponentially" (Turcotte, 1997: 219). This same fundamental characteristic of chaos is also called "sensitive dependence on initial conditions." To understand this concept, one can envision arbitrarily close orbits shooting off at wildly different trajectories. This is not stochastic behaviour. Chaotic behaviour occurs in systems that are completely determined. The fact that deterministic solutions can diverge exponentially means that even simple systems can behave in an unpredictable fashion. What happens, in fact, is that the behaviour of the system becomes mathematically unpredictable because any error or perturbation, no matter how small, propagates until it overwhelms the underlying pattern. The practical significance of chaotic behaviour is that prediction becomes impossible in the presence of chaos. This goes right to the heart of any philosophy of science that takes as its goal the discovery of predictive laws.

The relationship between fractals and chaos is of fundamental importance to archaeology. Fractals are the geometry of chaos (Peitgen, Harmut & Dietmar, 1992: 59). Strange attractors, which are the solution sets of chaotic systems, are fractals (Lorenz 1993: 176–178; Ruelle, 1991: 64). Fractals are the static trace of the orbits of chaotic dynamical systems. Therefore, in many contexts, fractals imply chaos. It is of course a dictum of modern archaeology that the archaeological record is the static picture of past cultural dynamics (e.g., Binford, 1981). If, then, some aspect of the static archaeological record is fractal, we may be able to infer that the original dynamical system that created the record was chaotic. Large and precise data sets are typically required to identify chaos in simple physical systems. Since such data sets are essentially unknown in archaeology, in which highly complex and poorly understood systems are the rule, fractals offer one means by which chaos can be recognized.

"Self-organized criticality" is another concept that links dynamical systems and fractals (Bak, 1996; Bak *et al.*, 1988). Certain non-linear dynamical systems exhibit self-organized criticality. "Criticality" refers to a marginally stable state toward which these systems spontaneously evolve. The classic model of this phenomenon is a sand pile to which sand is added one grain at a time. Eventually, the slope of the pile will reach a critical state—the angle of repose—after which the addition of more sand causes avalanches. Study of the avalanches indicates that they possess no natural scale and, thus, they exhibit fractal statistics in both space and time. The avalanches allow the system to evolve back to a critical state, where the further addition of sand will cause more avalanches. Thus, after perturbation, the system evolves back to marginal stability. The fractal characteristics of the avalanches of the theoretical sandpiles appear to explain several natural phenomena, including the fractal size-frequency distribution of geologic strata and the general fractality of erosional landscapes and hydrological systems (Bak, 1996: 80–84). Some physical systems, like meandering rivers, appear to unite all three concepts of fractals, chaos, and SOC: simulations of rivers indicate that the system evolves to a critical state that oscillates between stability and chaos (Stølum, 1996). For the reader thinking of archaeological and human systems, SOC will inspire not only explanations for site stratigraphy and taphonomy, or settlement patterns, but also systemic models of historic patterns, such as the rise and collapse of early states.

It may not be clear whether the fragmentation processes of archaeological lithic materials are either chaotic or SOC. Nevertheless, it is important that we use the mathematics and concepts of fractals in archaeology to explore non-linear processes in prehistory.

Acknowledgements

Sincerest thanks to: E. Wyllys Andrews V for advice, support, and funding; Dan Healan for teaching me about quantitative methods; Victoria R. Bricker for advice and much help; Chris Goodwin for advice, assistance and for giving me the opportunity to excavate Site 8HI483; R. Christopher Goodwin & Associates, Inc., and Florida Gas Transmission Company, Inc., for their gracious and generous support of the

research at Site 8HI473; the Consejo Técnico of the Instituto Nacional de Antropología e Historia (México) for permission to conduct research at Mayapán, Yucatán, and for the advice, assistance, hospitality, and great kindness of the archaeologists at the Centro Regional de Yucatán, particularly Tomás Gallareta N., Carlos Peraza L., Luis Millet C., Fernando Robles C., and Director Alfredo Barrera R.; Barbara Luedtke, Michael Coe, Kenneth Ashworth, and Craig Hanson for their comments and encouragement; Catherine T. Brown for much help, editorial advice and financial support; Jane Raskin for editorial advice and assistance; Walter R. T. Witschey for advice, encouragement and particularly inspiration, for he introduced me to the study of fractals; Stephen Ahler, Joel Gunn, and several anonymous reviewers for their comments; the National Science Foundation for Dissertation Improvement Grant DBS-9204580; and the Institute for International Education for a Fulbright grant.

References

Ahler, S. (1986). *The Knife River Flint Quarries: Excavations at Site 32DU508*. Bismark: State Historical Society of North Dakota.

Ahler, S. (1989). Mass analysis of flaking debris: studying the forest rather than the tree. In (D. O. Henry & G. H. Odell, Eds) *Alternative Approaches to Lithic Analysis*. Washington, D.C.: Archaeological Papers of the American Anthropological Association **1,** pp. 85–118.

Bak, P. (1996). *How Nature Works: The Science of Self-Organized Criticality*. New York: Springer-Verlag.

Bak, Per, Tang, C. & Wiesenfeld, K. (1988). Self-organized criticality. *Physical Review A* **38,** 364–374.

Barton, C. C. (1995). Fractal analysis of scaling and spatial clustering of fractures. In (C. C. Barton & P. R. LaPointe, Eds) *Fractals in the Earth Sciences*. New York: Plenum Press, pp. 141–178.

Batty, M. & Longley, P. (1994). *Fractal Cities*. New York: Academic Press.

Baumler, M. M. & Downum, C. E. (1989). Between micro and macro: a study in the interpretation of small-sized lithic debitage. In (D. S. Amick & R. Maudlin, Eds) *Experiments in Lithic Technology*. Oxford: B.A.R. International Series **528**, pp. 101–116.

Behm, J. A. (1983). Flake concentrations: distinguishing between flintworking activity areas and secondary deposits. *Lithic Technology* **12,** 9–16.

Binford, Lewis R. (1981). Behavioral archaeology and the "Pompeii premise". *Journal of Anthropological Research* **37,** 195–208.

Borodich, F. M. (1997). Some fractal models of fracture. *Journal of Mechanics and Physics of Solids* **45,** 239–259.

Brown, C. T. (1999). *Mayapán Society, and Ancient Maya Social Organization*. Ph.D. dissertation, Tulane University.

Brown, C. T., Darby, C. A., Green, J. A., Davies, C., Williams, M. L., Gordon, G., Vento, F. & Athens, W. P. (1995). *Phase III Data Recovery at Site 22PR533 for the Proposed Florida Gas Transmission Company Phase III Expansion Project, Pearl River County, Mississippi.* R. Christopher Goodwin & Associates, Inc., New Orleans. Submitted to Mississippi Department of Archives and History, Jackson, MS. Copies available from R. Christopher Goodwin & Associates, Inc.

Brown, C. T., Darby, C., Fenn, T., Davies, C., Green, J. A. Jr, Williams, M., Vento, F. & Athens, W. P. (1996). *Phase III Data Recovery at Sites 8HI473 and 8HI472/381 for the Proposed Florida Gas Transmission Company Phase III Expansion Project, Hillsborough County, Florida.* New Orleans: R. Christopher Goodwin & Associates, Inc. Submitted to the Florida Divsion of Historical Resources, Tallahassee, FL. Copies available from R. Christopher Goodwin & Associates, Inc.

Brown, S. R. (1995). Measuring the dimension of self-affine fractals: examples of rough surfaces. In (C. C. Barton & P. R. LaPointe, Eds) *Fractals in the Earth Sciences*. New York: Plenum Press, pp. 77–87.

Burlando, B. (1990). The fractal dimension of taxonomic systems. *Journal of Theoretical Biology* **146,** 99–114.

Burlando, B. (1993). The fractal geometry of evolution. *Journal of Theoretical Biology* **163,** 161–172.

Chance, M. A. (1982). *Phase II Investigations at Wetherington Island: A Lithic Procurement Site in Hillsborough County, Florida*. Interstate Highway 75 Phase II Archaeological Reports No. 3. Tallahassee: Bureau of Historic Sites and Properties, Florida Division of Archives, History and Records.

Chance, M. A. & Misner, E. J. (1984). *Archaic Lithic Procurement Behavior at Wetherington Island, Hillsborough County, Florida*. Tallahassee, FL: Report on file, Florida Bureau of Archaeological Research.

Clark, J. E. (1991*a*). Modern Lacandon lithic technology and blade workshops. In (T. R. Hester & H. J. Shafer, Eds) *Maya Stone Tools: Selected Papers from the Second Maya Lithic Conference*. Madison: Prehistory Press, Monographs in World Archaeology No. 1, pp. 251–266.

Clark, J. E. (1991*b*). Flintknapping and debitage disposal among the Lacandon Maya of Chiapas, Mexico. In (E. Staski & L. Sutro, Eds) *The Ethnoarchaeology of Refuse Disposal*. Tempe, AZ: Arizona State University Anthropological Research Papers No. 42, pp. 63–78.

Coutinho, K., Adhikari, S. K. & Gomes, M. A. F. (1993). Dynamic scaling in fragmentation. *Journal of Applied Physics* **74,** 7577–7587.

Fladmark, K. R. (1982). Microdebitage analysis: initial considerations. *Journal of Archaeological Science* **9,** 205–220.

Goodchild, M. F. & Mark, D. M. (1987). The fractal nature of geographic phenomena. *Annals of the Association of American Geographers* **77,** 265–278.

Goodyear, A. C., Upchurch, S. B., Brooks, M. J. & Goodyear, A. J. (1983). Paleo-Indian manifestations in the Tampa Bay Region, Florida. *Florida Anthropologist* **36,** 40–67.

Gunn, J., Mahula, R. & Sollberger, J. B. (1976). The Sollberger Distribution: analysis and application of a tool reduction sequence. *La Tierra* **3,** 2–8.

Healan, D. M. (1995). Identifying lithic reduction loci with size-graded macrodebitage: a multivariate approach. *American Antiquity* **60,** 689–699.

Henry, D. O., Haynes, C. V. & Bradley, B. (1976). Quantitative variations in flaked stone debitage. *Plains Anthropologist* **21,** 57–61.

Hirata, T. (1989). Fractal dimension of fault systems in Japan: fractal structure in rock fracture geometry at various scales. In (C. H. Scholz & B. B. Mandelbrot, Eds) *Fractals in Geophysics*. Basel: Birkhauser Verlag (reprinted from *Pure and Applied Geophysics* **131**), pp. 157–170.

Kalin, J. (1981). Stem point manufacture and debitage recovery. *Archaeology of Eastern North America* **9,** 134–175.

Kennedy, S. K. & Lin, W. (1986). Fract—A FORTRAN subroutine to calculate the variables necessary to determine the fractal dimension of closed forms. *Computers and Geosciences* **12,** 705–712.

Kennedy, S. K. & Lin, W. (1988). A fractal technique for the classification of projectile point shapes. *Geoarchaeology* **3,** 297–301.

Korvin, G. (1992). *Fractal Models in the Earth Sciences*. Amsterdam: Elsevier.

Lorenz, E. N. (1993). *The Essence of Chaos*. Seattle: University of Washington Press.

Luedtke, B. E. (1992). *An Archaeologist's Guide to Chert and Flint*. Archaeological Research Tools 7. Los Angeles: Institute of Archaeology, University of California.

Mandelbrot, B. B. (1967). How long is the coast of Britain? Statistical self-similarity and fractional dimension. *Science* **156,** 636–638.

Mandelbrot, B. B. (1983). *The Fractal Geometry of Nature*. Revised edition. New York: W. H. Freeman and Company.

McDowell, G. R., Bolton, M. D. & Robertson, D. (1996). The fractal crushing of granular materials. *Journal of Mechanical Physics and Solids* **44,** 2079–2102.

Mecholsky, J. J. & Mackin, T. J. (1988). Fractal analysis of fracture in Ocala chert. *Journal of Materials Science Letters* **7,** 1145–1147.

Mekjian, A. Z. (1990). Model of a fragmentation process and its power-law behavior. *Physical Review Letters* **64,** 2125–2128.

Patterson, L. (1990). Characteristics of Bifacial-Reduction Flake-Size Distribution. *American Antiquity* **55,** 550–558.

Peitgen, H.-O., Harmut, J. & Dietmar, S. (1992). *Chaos and Fractals: New Frontiers of Science*. New York: Springer-Verlag.

Proskouriakoff, T. (1962). Part 4: The artifacts of Mayapán. In (H. E. D. Pollock, R. L. Roys, T. Proskouriakoff & A. L. Smith) *Mayapan, Yucatan, Mexico*. Washington: Carnegie Institution of Washington, Publication No. **619**, pp. 321–442.

Root, M. J. (1997). Production for exchange at the Knife River Flint Quarries, North Dakota. *Lithic Technology* **22,** 33–50.

Ruelle, D. (1991). *Chance and Chaos*. Princeton: Princeton University Press.

Schroeder, M. (1991). *Fractals, Chaos, Power Laws: Minutes from an Infinite Paradise*. New York: W. H. Freeman and Company.

Shott, M. J. (1994). Size and form in the analysis of flake debris: review and recent approaches. *Journal of Archaeological Method and Theory* **1,** 69–110.

Smith, A. L. (1962). Residential and associated structures at Mayapan. In (H. E. D. Pollock, R. L. Roys, T. Proskouriakoff & A. L. Smith) *Mayapan, Yucatan, Mexico*. Washington, D.C.: Carnegie Institution of Washington, Publication No. **619**, pp. 165–313.

Stahle, D. W. & Dunn, J. E. (1982). An analysis and application of the size distribution of waste flakes from the manufacture of bifacial stone tools. *World Archaeology* **14,** 98–119.

Stahle, D. W. & Dunn, J. E. (1984). An experimental analysis of the size distribution of waste flakes from biface reduction. *Arkansas Archaeological Survey Technical Paper* No. **2**.

Steacy, S. & Sammis, C. G. (1991). An automaton for fractal patterns of fragmentation. *Nature* **353,** 250–252.

Stølum, Hans-Henrik (1996). River meandering as a self-organization process. *Science* **271,** 1710–1713.

Turcotte, D. L. (1986). Fractals and fragmentation. *Journal of Geophysical Research* **91,** 1921–1926.

Turcotte, D. L. (1997). *Fractals and Chaos in Geology and Geophysics*. Second edition. Cambridge: Cambridge University Press.

Turcotte, D. L. & Huang, J. (1995). Fractal distributions in geology, scale invariance, and deterministic chaos. In (C. C. Barton & P. R. LaPointe, Eds) *Fractals in the Earth Sciences*. New York: Plenum Press, pp. 1–40.

Villemin, T., Angelier, J. & Sunwoo, C. (1995). Fractal distribution of fault length and offsets: implications of brittle deformation evaluation—The Lorraine Coal Basin. In (C. C. Barton & P. R. LaPointe, Eds) *Fractals in the Earth Sciences*. New York: Plenum Press, pp. 205–226.

Weibull, W. (1951). A statistical distribution of wide applicability. *Journal of Applied Mechanics* **18,** 293–297.